Non-tidal ocean loading effects on geodetic GPS heights

S. D. P. Williams[1] and N. T. Penna[2]

Received 28 January 2011; revised 1 April 2011; accepted 3 April 2011; published 11 May 2011.

[1] GPS observations used in geophysical studies are not usually corrected for non-tidal ocean loading (NTOL) displacement. Here we investigate NTOL effects on 3–4 year GPS height time series from 17 sites around the southern North Sea, and compute the NTOL displacement according to two ocean models; the global ECCO model and a high resolution regional model, POLSSM, which covers the northwest European continental shelf. To assess the susceptibility of GPS height estimates to NTOL, reprocessed GIPSY PPP daily solutions are corrected for the resulting displacement, together with atmospheric pressure loading (ATML). We find that the displacements due to NTOL are comparable in size to ATML and the combined correction reduces the variance by 12–22 mm^2 (20–30% reduction in RMS). We find that POLSSM outperforms ECCO, with around an 11% greater variance reduction, and hence high resolution models are recommended to correct GPS heights for NTOL. **Citation:** Williams, S. D. P., and N. T. Penna (2011), Non-tidal ocean loading effects on geodetic GPS heights, *Geophys. Res. Lett.*, *38*, L09314, doi:10.1029/2011GL046940.

1. Introduction

[2] Long-term geophysical processes such as sea level change, tectonic motion and glacial isostatic adjustment may be measured using geodetic GPS coordinate time series. To enable such (sub-) millimeter per year order motions to be confidently identified, shorter-term deformation time series signatures caused by loading of the surface of the solid Earth from the constant redistribution of atmospheric, oceanic and continental-water masses, must be removed from the time series with suitably accurate geophysical models. Ocean tide loading displacements are routinely corrected in geodetic data processing with recent models agreeing to around 1 mm or better in all but a few regions of the world [*Penna et al.*, 2008]. Atmospheric pressure loading (ATML) predictions, following their introduction over 20 years ago, are now provided by several on-line services either as corrections at known geodetic sites or in the form of global grids. *van Dam et al.* [1994] found that removing modeled ATML from GPS heights reduced the variance at 12 of 19 globally-distributed sites and that ATML could account for up to 24% of the total variance, and later *Tregoning and van Dam* [2005] showed peak to peak vertical displacements of up to 18 mm for mid-to-high latitude sites and a reduction in RMS of up to 2 mm. However, GPS time series are not normally corrected for loading effects of non-tidal water redistributions, possibly due to the lack of temporal (monthly for continental water and 12 hourly for ocean) and spatial (1° or coarser) resolution of readily accessible models and their estimated contribution is still a subject of debate, with only limited, or somewhat inconclusive, studies undertaken. Using TOPEX/POSEIDON (T/P) altimeter data and output from an oceanic general circulation model to infer changes in ocean bottom pressure, *van Dam et al.* [1997] found a typical site RMS of 2 mm in the modeled height displacements for sites close to the coast. *Munekane and Matsuzaka* [2004] found evidence that some vertical movement at three tropical Pacific island GPS sites was anti-correlated with T/P altimeter data corrected for steric effects. A reduction in height variance of about 10% for four GPS sites (corrected for ATML) around the Adriatic region was shown by *Zerbini et al.* [2004] on applying non-tidal ocean loading (NTOL) displacements computed using the Estimating the Circulation and Climate of the Oceans (ECCO) model, but the modeled and observed NTOL differed by a scaling factor of about 2.5. *Nordman et al.* [2009], using interpolated monthly sea level data from Baltic tide gauges to compute NTOL, found an improvement in RMS at only one of their three Fennoscandia GPS sites and when ATML predictions were also added, they found no overall decrease in RMS. Both *Zerbini et al.* [2004] and *Nordman et al.* [2009] used 'legacy' GPS analysis methods, notably using inhomogeneously computed International GNSS Service (IGS)/Jet Propulsion Laboratory (JPL) orbits respectively, rather than homogeneous reprocessing incorporating updated error models. *Wöppelmann et al.* [2009] for example, found reductions in the noise of such height time series of 30–40% compared with 'legacy' processing.

[3] This paper investigates whether NTOL effects on geodetic GPS height time series are significant and should (and can) be modeled in geophysical studies, by considering modeled displacements and 3–4 years of homogeneously reprocessed GPS data using current error models. We consider 17 coastal EUREF (www.epncb.oma.be) and NERC BIGF (www.bigf.ac.uk) sites around the southern North Sea (Figure 1), a region particularly susceptible to storm surges, and investigate whether global, coarse spatial and temporal resolution ocean models are adequate, or whether finer resolution regional models are preferred. As NTOL is correlated with atmospheric pressure, we also consider atmospheric pressure loading (ATML) effects, and the coupling between NTOL and ATML. As a spin-off, the changes in the precision of the GPS height time series also enable us to assess the quality of the ocean models themselves.

2. Modeling Atmospheric and Non-tidal Ocean Loading Displacements

2.1. Model Data

[4] To compute the ATML we used the surface pressure fields from the National Centers for Environmental Prediction/

[1]National Oceanography Centre, Liverpool, UK.
[2]School of Civil Engineering and Geosciences, Newcastle University, Newcastle upon Tyne, UK.

0094-8276/11/2011GL046940

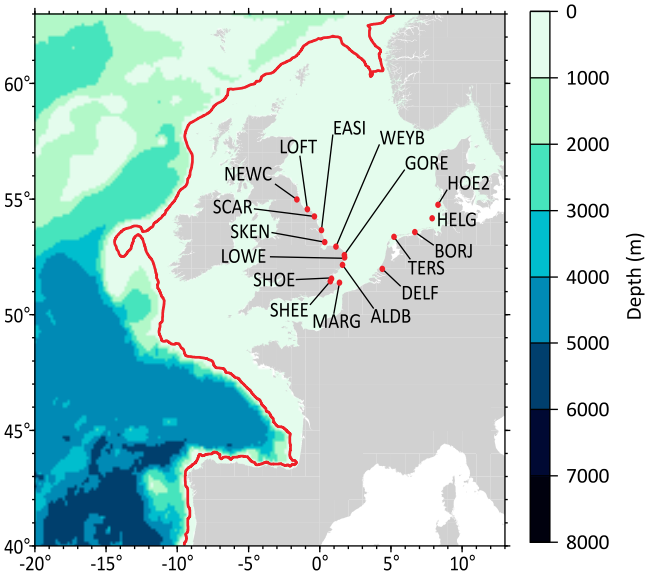

Figure 1. Regional extent of the extended POLSSM model. The red line indicates the 300 m ocean depth contour, with all ocean depths denoted by colors. Red dots denote the locations of the 17 GPS sites within 15 km of the southern North Sea coast used in this study.

National Center for Atmospheric Research (NCEP/NCAR) reanalysis project [*Kalnay et al.*, 1996]. The dataset consists of a global grid with a 2.5° × 2.5° spatial and a 6-hourly temporal resolution. We handled the problematic S_1 and S_2 atmospheric tides [*Ponte and Ray*, 2002] by calculating and removing the 30 year (1978–2008) mean for each 6 hourly time step (00 h, 06 h, 12 h, 18 h). This is exactly equivalent, in a weighted least squares sense, to estimating and removing the mean pressure, sine and cosine amplitudes of the S_1 tide and the cosine of the S_2 tide over the entire period; the approach taken by *Petrov and Boy* [2004].

[5] To compute the NTOL we used the output from two different models, a near global ocean circulation model and a high resolution storm surge model restricted to the northwest European continental shelf. The first model we tested uses the ocean bottom pressure output from model kf066b, a data assimilated oceanic general circulation model run at JPL as part of the ECCO consortium [*Stammer et al.*, 2002]. The model extends between ±80° latitude with a longitudinal grid spacing of 1°, and a latitudinal grid spacing of 0.3° within 10° of the equator that gradually increases to a 1° resolution at ±25°. It is provided at 12 hour sampling, with the values representing an average over 12 hours rather than an instantaneous snapshot. Sea level observations from satellite altimetry are assimilated into the model using a Kalman filter approach [*Fukumori et al.*, 1999] and the models are forced with wind stress, surface heat flux and evaporation-precipitation fields from the NCEP/NCAR reanalysis. The model uses the Boussinesq approximation that conserves volume rather than mass. This can produce unwanted spurious effects which can be reduced by calculating and removing the global mean bottom pressure at each epoch [*Greatbatch*, 1994].

[6] For a second approach to modeling the NTOL we used the UK operational tide-storm surge model, POLSSM (Proudman Oceanographic Laboratory Storm Surge Model), which covers the entire northwest European continental shelf from 40°N to 63°N and from 20°W to 13°E (Figure 1) at 12 km spatial and 1 hour temporal resolution [*Flather*, 2000]. The surface boundary conditions for this barotropic model are the mean sea level atmospheric pressure and 10 m wind components. Validation of the operational model is performed monthly by comparison with observed sea level data from the UK national tide gauge network and typical RMS errors are about 10 cm.

2.2. Loading Computation

[7] The loading was calculated by convolving the atmospheric and non-tidal ocean models with the Green's function for the PREM model, as described by *Farrell* [1972]. We used the SPOTL [*Agnew*, 1997] program, which uses a polar grid centered on the station with grid dimensions increasing with distance from the center. We used degree one Love numbers such that the implied frame is the center of mass of the solid Earth (CE) [*Blewitt*, 2003].

[8] The ECCO model does not include atmospheric pressure forcing, of which the primary response in the oceans is an inverted barometer (IB) at time scales greater than a few days. Traditionally, the modified IB effect, whereby the net change in mass above the oceans is applied evenly across the whole ocean floor [*van Dam and Wahr*, 1987], has been applied to the ATML calculations. Therefore for continuity and to facilitate comparison with previous ATML datasets, we attribute this effect to the ATML and not the NTOL induced effect. A comparison between our ATML displacement time series and those calculated by *Petrov and Boy* [2004] at six European sites showed a maximum standard deviation of the differences of 0.07, 0.03 and 0.3 mm in north, east and up respectively.

[9] In order to embed the regional POLSSM ocean model in what is essentially a global calculation we must be conscious of global mass conservation. While the dynamics within the model are well defined, the total mass on the shelf is sensitive to the applied open-ocean boundary condition, which is ignorant of global mass conservation. To achieve this we took advantage of the fact that there is a minimum of sea level variability (and, by implication, bottom pressure variability) near the steepest part of the continental slope, leading to a decoupling of deep ocean and shelf sea variability [*Hughes and Williams*, 2010]. We assumed that the model correctly represents bottom pressure gradients on the shelf, which we defined as the region shallower than 300 m, but that the bottom pressure gradient is zero in the global ocean outside this depth contour, the latter being equivalent to the usual assumption of a passive IB ocean. At each epoch, we then added a separate, spatially-uniform bottom pressure in order to ensure conservation of global ocean mass, and continuity of the bottom pressure signal averaged along the 300 m contour. This strategy did however necessitate that the ATML and NTOL calculations are not entirely separate (they are for the two global grids), meaning that the ATML is slightly different from that associated with the ECCO model.

3. GPS Processing

[10] For the 17 North Sea sites considered, all available GPS data during the window 2005.0 to 2009.0 were processed in daily 24 hour batches using the GIPSY v5.0 software in

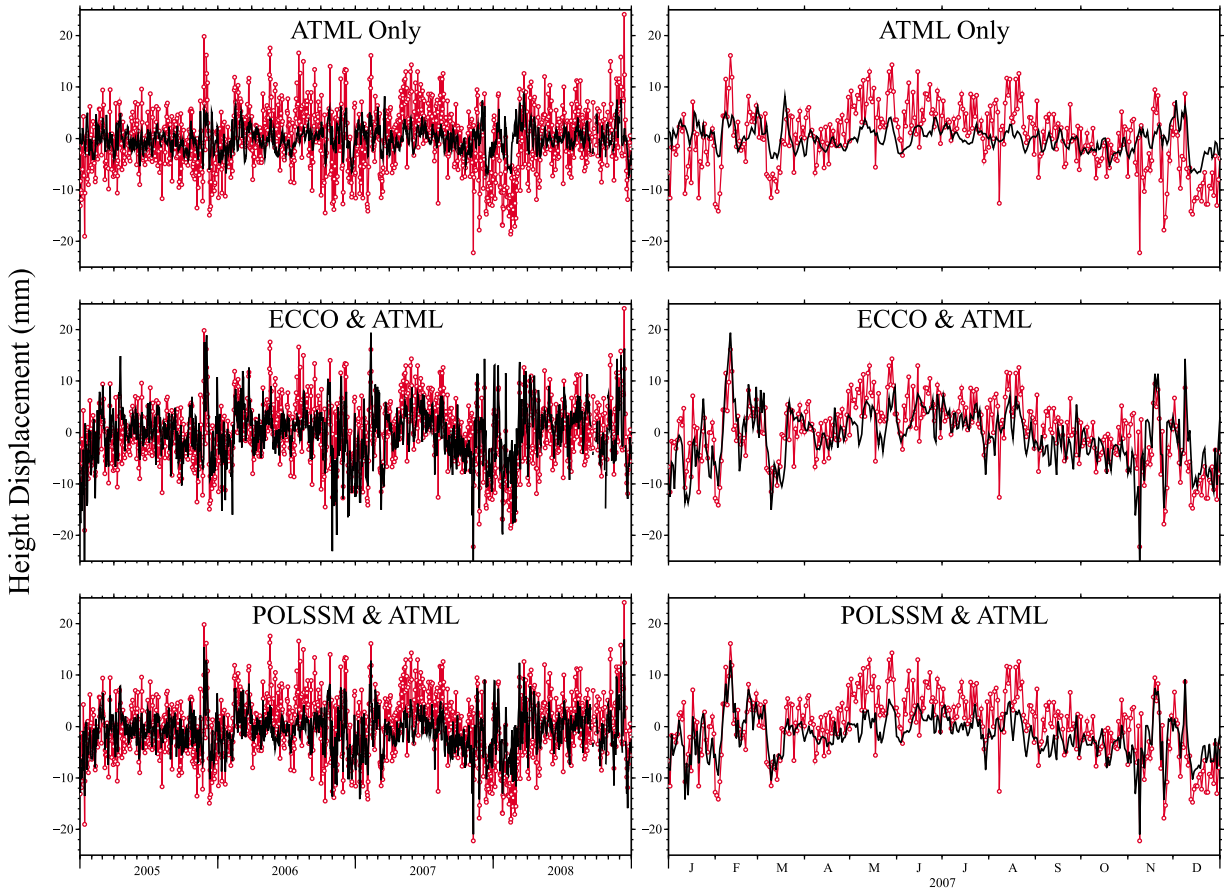

Figure 2. Observed GPS height time series (red) and modeled loading displacement (black) for the site TERS (left) over the 4 year time span 2005.0–2009.0 and (right) over 1 year, 2007. (top) Modeled displacement due to ATML only. (middle) Combined displacement due to ATML and NTOL calculated from the ECCO model. (bottom) Combined displacement due to ATML and NTOL calculated from the POLSSM model.

precise point positioning mode [*Zumberge et al.*, 1997]. JPL reprocessed fiducial-free satellite orbit and clock products were held fixed, estimating one set of coordinates per 24 hour batch, together with receiver clock offsets (white noise) and tropospheric zenith residual delays (to ECMWF-derived a priori hydrostatic and wet zenith delays) and north-south and east-west gradients every 5 minutes. Random walk sigmas of 3 mm/√h and 0.3 mm/√h were applied in the zenith delay and gradient estimation, respectively. The VMF1 [*Boehm et al.*, 2006] tropospheric mapping function and a 10 degree elevation cut-off were used, with absolute satellite and receiver antenna phase centre variations and offsets modeled according to *Schmid et al.* [2007], and ocean tide loading displacement corrections (computed using SPOTL and the FES2004 [*Lyard et al.*, 2006] ocean tide model) applied. Ambiguities were fixed using ambizap v3 [*Blewitt*, 2008], which rejects a site on a day if less than 18 hours data are available. The resulting daily height estimates were transformed to the IGS realization of ITRF2005 and concatenated to form the homogeneously reprocessed (observed) GPS height time series, typically 3–4 years long per site.

4. Results

[11] The observed GPS height time series for an example site, TERS, is shown in Figure 2. Also included are the daily averages of the ATML displacement and the combined ATML and NTOL displacement from both the ECCO and POLSSM models. Visually there is a good agreement between the observed and predicted displacements, although the displacement predicted from the global ECCO model appears larger than that predicted from the regional POLSSM model. To assess the effectiveness of the loading models on the GPS height time series we use the statistical techniques of *van Dam and Herring* [1994] and *van Dam et al.* [1994]. The GPS height variance changes are shown in Table 1 for six different scenarios: (i) the predicted ATML is removed; (ii) the predicted NTOL is removed; (iii) the NTOL is removed after the ATML has been removed from the GPS heights first; (iv) the ATML is removed after the NTOL has been removed from the GPS heights first; (v) both the ATML and the NTOL are removed; (vi) both loads are removed after applying scaling parameters that maximize the variance change. Scenario (iii) illustrates how much extra variance reduction the NTOL creates over the more standard ATML calculation and scenario (iv) illustrates how much extra variance ATML creates over the NTOL. We find that the variance has been reduced in all cases except one, namely scenario (ii) for the ECCO model at site BORJ. A typical estimate of the uncertainty in the variance change is about 0.4 to 1.5 mm^2 and all variance changes except three are significant at the three sigma

Table 1. Variance Change to the Observed 3–4 Year GPS Height Time Series After Removing Displacements From Various Loading Components[a]

Site	Distance From Coast (km)	Number of Points	GPS Height Variance (mm^2)	Variance Change (mm^2)											
				ECCO Model						POLSSM Model					
				ATML[b]	NTOL[c]	N−A[d]	A−N[e]	A+N[f]	Scaled[g]	ATML	NTOL	N−A	A−N	A+N	Scaled
NEWC	11.3	1397	35.8	10.4	3.8	1.3	7.9	11.7	12.8	10.8	5.0	2.5	8.3	13.3	13.4
LOFT	0.9	1123	43.7	8.9	10.3	6.8	5.3	15.7	15.8	9.2	10.4	7.2	6.1	16.5	17.0
SCAR	0.8	1400	38.1	9.4	10.3	7.5	6.6	16.9	17.1	10.0	9.9	7.4	7.4	17.3	17.9
EASI	0.9	1393	38.6	10.9	9.0	6.1	8.0	17.0	18.2	11.5	10.6	8.1	9.0	19.6	20.5
SKEN	0.4	1015	40.3	12.1	9.4	5.6	8.4	17.7	18.3	12.7	9.9	6.6	9.4	19.3	19.6
WEYB	0.7	1380	31.9	7.5	6.1	3.9	5.3	11.4	12.7	8.1	6.8	4.8	6.1	12.9	13.0
GORE	0.4	1271	33.9	8.9	9.2	6.3	6.0	15.2	16.1	9.6	9.9	7.5	7.1	17.0	17.1
LOWE	0.2	1285	32.9	8.3	7.7	5.1	5.7	13.4	14.7	9.0	9.3	6.8	6.6	15.8	15.8
ALDB	0.2	882	33.6	8.3	10.2	6.6	4.7	14.8	15.5	9.1	9.9	6.8	6.0	15.9	16.0
SHOE	1.4	1175	33.8	9.8	3.9	2.1	8.0	11.9	12.1	10.4	5.6	3.2	8.0	13.6	13.6
SHEE	0.1	1147	47.0	11.9	3.8	2.5	10.5	14.3	14.7	12.6	5.9	3.7	10.4	16.3	16.6
MARG	0.1	1380	28.6	8.3	4.5	3.1	6.9	11.4	11.5	8.7	4.7	3.1	7.1	11.9	12.0
DELF	14.8	1458	36.3	9.7	6.3	5.2	8.6	14.9	15.3	10.6	5.6	5.1	10.0	15.6	16.0
TERS	0.1	1439	34.8	6.4	6.5	7.0	6.8	13.4	16.6	7.0	10.2	10.9	7.7	17.9	18.1
BORJ	0.1	1263	37.3	8.8	−1.2	3.1	13.2	12.0	18.0	9.5	8.8	10.1	10.8	19.6	20.0
HELG	0.1	1418	43.1	2.7	12.4	16.4	6.8	19.1	20.0	3.5	15.4	18.7	6.8	22.2	22.7
HOE2	0.2	1242	35.6	6.7	5.5	9.1	10.3	15.8	17.2	7.4	7.9	11.6	11.1	19.0	19.4
Median			35.8	8.9	6.5	5.6	6.9	14.8	15.8	9.5	9.3	6.8	7.7	16.5	17.0
RMS Reduction (%)				13.5	10.1	10.6	13.1	23.0	25.8	14.6	12.7	14.1	15.4	27.5	27.7
Correlation Coefficient				0.51	0.48	0.49	0.50	0.66	0.67	0.53	0.53	0.53	0.53	0.64	0.69

[a]A positive change indicates a reduction in variance. Also shown are the median variance change, median RMS reduction (in percent) and the median correlation coefficients between the observed GPS heights and loading displacement.
[b]Atmospheric loading component removed.
[c]Non-tidal ocean loading removed.
[d]Variance change due to non-tidal ocean loading after atmospheric loading component has already been removed.
[e]Variance change due to atmospheric loading after non-tidal ocean loading component has already been removed.
[f]Atmospheric and non-tidal ocean loading components removed.
[g]Atmospheric and non-tidal ocean loading components removed after scaling.

confidence level. Also shown in Table 1 are the median variance changes for the 17 sites, the median percentage reduction in RMS and the median correlation coefficients between the modeled series and the GPS observations.

[12] In all the outlined scenarios, the POLSSM model outperforms the ECCO model by around 11%. The reduction in variance is slightly bigger for the ATML component than the NTOL but the variance reduction is clearly improved if both loads are applied together, with a median change of 17 mm^2 for the POLSSM model, ranging from 12 to 22 mm^2 (over 50% in some cases).

[13] In scenario (vi) the median estimated scale parameter for the ATML is 1.1 for both ECCO and POLSSM. For the NTOL the median scaling parameter is 0.8 for the ECCO model and leads to an improvement, with the variance reduction rising by 1 mm^2. This would appear to indicate that the ECCO model is over predicting the bottom pressure, and hence displacements, in this region by about 30% (as observed in Figure 2). The coarse resolution of the ECCO model also means that the eastern half of the English Channel is missing and hence nearby sites such as MARG, SHEE and SHOE are only loaded by distant grid points. It is not very noticeable in the results but that may be because the missing ocean partially compensates for the over prediction of the loading. For POLSSM the NTOL scaling parameter indicates that the displacements are under predicted by about 10% and we find a variance reduction increase of around 0.5 mm^2.

5. Discussion and Conclusions

[14] We have shown that geodetic homogeneously reprocessed GPS height time series for sites around the southern North Sea exhibit NTOL effects of comparable size to ATML. For island sites such as HELG and TERS the NTOL variance reduction is greater than that due to ATML (over 4 times greater for HELG). For more inland sites such as NEWC, DELF and sites situated within estuaries or bays, the ATML is dominant. Together, NTOL and ATML can reduce the GPS height variance by 12 to 22 mm^2 (35–54%), much greater than the negligible improvement reported by *Nordman et al.* [2009], and equivalent to an RMS reduction of around 20–30%. The variance reduction arising from NTOL, having already removed ATML, reaches up to 44% (for HELG), much greater than the 10% reductions reported by *Zerbini et al.* [2004]. Clearly NTOL corrections should be applied to GPS measurements used in geophysical studies, but which is not normally undertaken by GPS analysts, including key geophysical providers such as the IGS Analysis Centers, even in their reprocessing. Implementing such corrections will decrease the time required to detect changes in mean sea level, improve our ability to measure transients, and increase the correlation between GPS and GRACE-based estimates of elastic deformation due to hydrological loading [e.g., *Tregoning et al.*, 2009].

[15] Maximum geophysical benefit of GPS measurements will only be obtained (at least for shallow seas such as the southern North Sea) if NTOL effects are removed using high resolution models such as POLSSM (12 km grid), although such models are not readily available. We have demonstrated that the global 1° grid ECCO model (kf066b) can provide a useful first order approach, although the displacements had to be scaled by 0.8 to maximize the height time series variance reduction and hence the ECCO model overpredicts NTOL in the southern North Sea (*Zerbini et al.*

[2004] had to do an equivalent scaling of about 2.5 for Adriatic GPS sites processed using 'legacy' orbits and procedures rather than the updated reprocessed GPS analysis used here). Meanwhile, for POLSSM the overall variance reduction was 11% greater than when using ECCO, and at sites TERS and BORJ the reductions were improved by 33% and 63% respectively. These results highlight the usefulness of a high-resolution model (even if lacking in global coverage) compared to a low-resolution global model. The results also provide integrated checks on the ocean models using an independent dataset, which could be used to help refine such models in the future.

[16] **Acknowledgments.** We are grateful to NASA JPL for the provision of the GIPSY v5.0 software and orbit/clock products, and to EUREF and NERC BIGF (www.bigf.ac.uk) for GPS data. Thanks to Chris Hughes for many helpful discussions, to Kevin Horsburgh for access to POLSSM, to Geoff Blewitt for the provision of ambizap3, to Duncan Agnew for the SPOTL software and to Rory Bingham for comments on an earlier version of the manuscript. The figures were generated using the GMT software [*Wessel and Smith*, 1998].

[17] The Editor thanks two anonymous reviewers for their assistance in evaluating this paper.

References

Agnew, D. C. (1997), NLOADF: A program for computing ocean-tide loading, *J. Geophys. Res.*, *102*(B3), 5109–5110, doi:10.1029/96JB03458.

Blewitt, G. (2003), Self-consistency in reference frames, geocenter definition, and surface loading of the solid Earth, *J. Geophys. Res.*, *108*(B2), 2103, doi:10.1029/2002JB002082.

Blewitt, G. (2008), Fixed point theorems of GPS carrier phase ambiguity resolution and their application to massive network processing: Ambizap, *J. Geophys. Res.*, *113*, B12410, doi:10.1029/2008JB005736.

Boehm, J., B. Werl, and H. Schuh (2006), Troposphere mapping functions for GPS and very long baseline interferometry from European Centre for Medium-Range Weather Forecasts operational analysis data, *J. Geophys. Res.*, *111*, B02406, doi:10.1029/2005JB003629.

Farrell, W. E. (1972), Deformation of the Earth by surface loads, *Rev. Geophys.*, *10*, 761–797, doi:10.1029/RG010i003p00761.

Flather, R. A. (2000), Existing operational oceanography, *Coastal Eng.*, *41*, 13–40, doi:10.1016/S0378-3839(00)00025-9.

Fukumori, I., R. Raghunath, L. Fu, and Y. Chao (1999), Assimilation of TOPEX/POSEIDON data into a global ocean circulation model: How good are the results?, *J. Geophys. Res.*, *104*(C11), 25,647–25,665, doi:10.1029/1999JC900193.

Greatbatch, R. J. (1994), A note on the representation of steric sea level in models that conserve volume rather than mass, *J. Geophys. Res.*, *99*, 12,767–12,771, doi:10.1029/94JC00847.

Hughes, C. W., and S. D. P. Williams (2010), The color of sea level: Importance of spatial variations in spectral shape for assessing the significance of trends, *J. Geophys. Res.*, *115*(C6), C10048, doi:10.1029/2010JC006102.

Kalnay, E., et al. (1996), The NCEP/NCAR 40-year reanalysis project, *Bull. Am. Meteorol. Soc.*, *77*, 437–471, doi:10.1175/1520-0477(1996)077<0437:TNYRP>2.0.CO;2.

Lyard, F., F. Lefevre, T. Letellier, and O. Francis (2006), Modelling the global ocean tides: Modern insights from FES2004, *Ocean Dyn.*, *56*, 394–415, doi:10.1007/s10236-006-0086-x.

Munekane, H., and S. Matsuzaka (2004), Nontidal ocean mass loading detected by GPS observations in the tropical Pacific region, *Geophys. Res. Lett.*, *31*, L08602, doi:10.1029/2004GL019773.

Nordman, M., J. Mäkinen, H. Virtanen, J. M. Johansson, M. Bilker-Koivula, and J. Virtanen (2009), Crustal loading in vertical GPS time series in Fennoscandia, *J. Geodyn.*, *48*, 144–150, doi:10.1016/j.jog.2009.09.003.

Penna, N. T., M. S. Bos, T. F. Baker, and H.-G. Scherneck (2008), Investigating the accuracy of predicted ocean tide loading displacement values, *J. Geod.*, *82*(12), 893–907, doi:10.1007/s00190-008-0220-2.

Petrov, L., and J.-P. Boy (2004), Study of the atmospheric pressure loading signal in very long baseline interferometry observations, *J. Geophys. Res.*, *109*, B03405, doi:10.1029/2003JB002500.

Ponte, R. M., and R. D. Ray (2002), Atmospheric pressure corrections in geodesy and oceanography: A strategy for handling air tides, *Geophys. Res. Lett.*, *29*(24), 2153, doi:10.1029/2002GL016340.

Schmid, R., P. Steigenberger, G. Gendt, M. Ge, and M. Rothacher (2007), Generation of a consistent absolute phase center correction model for GPS receiver and satellite antennas, *J. Geod.*, *81*(12), 781–798, doi:10.1007/s00190-007-0148-y.

Stammer, D., C. Wunsch, I. Fukumori, and J. Marshall (2002), State estimation in modern oceanographic research, *Eos Trans. AGU*, *83*(27), 294–295, doi:10.1029/2002EO000207.

Tregoning, P., and T. van Dam (2005), Atmospheric pressure loading corrections applied to GPS data at the observation level, *Geophys. Res. Lett.*, *32*, L22310, doi:10.1029/2005GL024104.

Tregoning, P., C. Watson, G. Ramillien, H. McQueen, and J. Zhang (2009), Detecting hydrologic deformation using GRACE and GPS, *Geophys. Res. Lett.*, *36*, L15401, doi:10.1029/2009GL038718.

van Dam, T. M., and T. Herring (1994), Detection of atmospheric pressure loading using very long baseline interferometry measurements, *J. Geophys. Res.*, *99*(B3), 4505–4517, doi:10.1029/93JB02758.

van Dam, T. M., and J. Wahr (1987), Displacements of the Earth's surface due to atmospheric loading: Effects on gravity and baseline measurements, *J. Geophys. Res.*, *92*(B2), 1281–1286, doi:10.1029/JB092iB02p01281.

van Dam, T. M., G. Blewitt, and M. B. Heflin (1994), Atmospheric pressure loading effects on Global Positioning System coordinate determinations, *J. Geophys. Res.*, *99*(B12), 23,939–23,950, doi:10.1029/94JB02122.

van Dam, T. M., J. Wahr, Y. Chao, and E. Leuliette (1997), Predictions of crustal deformation and of geoid and sea-level variability caused by oceanic and atmospheric loading, *Geophys. J. Int.*, *129*, 507–517, doi:10.1111/j.1365-246X.1997.tb04490.x.

Wessel, P., and W. H. F. Smith (1998), New, improved versions of the Generic Mapping Tools released, *Eos Trans. AGU*, *79*(47), 579, doi:10.1029/98EO00426.

Wöppelmann, G., C. Letetrel, A. Santamaria, M.-N. Bouin, X. Collilieux, Z. Altamimi, S. D. P. Williams, and B. Martin Miguez (2009), Rates of sea-level change over the past century in a geocentric reference frame, *Geophys. Res. Lett.*, *36*, L12607, doi:10.1029/2009GL038720.

Zerbini, S., F. Matonti, F. Raicich, B. Richter, and T. van Dam (2004), Observing and assessing non tidal ocean, continuous GPS and gravity data in the Adriatic area, *Geophys. Res. Lett.*, *31*, L23609, doi:10.1029/2004GL021185.

Zumberge, J. F., M. B. Heflin, D. C. Jefferson, M. M. Watkins, and F. H. Webb (1997), Precise point positioning for the efficient and robust analysis of GPS data from large networks, *J. Geophys. Res.*, *102*(B3), 5005–5017, doi:10.1029/96JB03860.

N. T. Penna, School of Civil Engineering and Geosciences, Newcastle University, Newcastle upon Tyne NE1 7RU, UK.

S. D. P. Williams, National Oceanography Centre, Liverpool, Joseph Proudman Building, 6 Brownlow St., Liverpool L3 5DA, UK. (sdwil@pol.ac.uk)